RESEARCH ARTICLE

Lysophosphatidic Acid (LPA) and Its Receptor, LPA_1, Influence Embryonic Schwann Cell Migration, Myelination, and Cell-to-Axon Segregation

Brigitte Anliker,[1] Ji Woong Choi,[2] Mu-En Lin,[1] Shannon E. Gardell,[1] Richard R. Rivera,[1] Grace Kennedy,[1] and Jerold Chun[1]

Schwann cell (SC) migration is an important step preceding myelination and remyelination in the peripheral nervous system, and can be promoted by peptide factors like neuregulins. Here we present evidence that a lipid factor, lysophosphatidic acid (LPA), influences both SC migration and peripheral myelination through its cognate G protein-coupled receptor (GPCR) known as LPA_1. Ultrastructural analyses of peripheral nerves in mouse null-mutants for LPA_1 showed delayed SC-to-axon segregation, polyaxonal myelination by single SCs, and thinner myelin sheaths. In primary cultures, LPA promoted SC migration through LPA_1, while analysis of conditioned media from purified dorsal root ganglia neurons using HPLC/MS supported the production of LPA by these neurons. The heterotrimeric G-alpha protein, $G_{\alpha i}$, and the small GTPase, Rac1, were identified as important downstream signaling components of LPA_1. These results identify receptor mediated LPA signaling between neurons and SCs that promote SC migration and contribute to the normal development of peripheral nerves through effects on SC-axon segregation and myelination.

GLIA 2013;61:2009–2022

Key words: LPA, Schwann cell, Rac1, G_i, myelination

Introduction

In order to establish a 1:1 relationship between ensheathing Schwann cells (SCs), the myelinating glia of the peripheral nervous system (PNS), and axons during myelination, SCs must go through necessary developmental and differentiation steps (Jessen and Mirsky, 2005). Several peptidergic signals have been reported to control SC proliferation, migration, and differentiation as well as the myelination process itself. These signaling molecules include neuregulin-1 (NRG) and brain-derived neurotrophic factor (BDNF) that signal through ErbB2/ErbB3 receptor tyrosine kinases (Garratt et al., 2000; Lemke, 2006; Michailov et al., 2004; Nave and Salzer, 2006) and the $p75^{NTR}$ receptor (Chan et al., 2001; Cosgaya et al., 2002; Yamauchi et al., 2004), respectively.

In addition to these peptide signals, the expression of LPA_1 in myelinating cells has also suggested a role for the bioactive phospholipid, lysophosphatidic acid (LPA), in myelination (Allard et al., 1998; Cervera et al., 2002; Contos et al., 2000; Weiner et al., 1998). LPA signaling in SCs has been demonstrated to alter the actin cytoskeleton and regulate cell adhesion (Weiner et al., 2001), as well as reduce SC apoptosis in the sciatic nerve (Contos et al., 2000; Weiner and Chun, 1999). LPA_1 was shown to influence myelination through over-activation of the Rho/ROCK pathway during the induction of neuropathic pain, a process that includes demyelination in the PNS (Inoue et al., 2004). Demyelination is associated with dedifferentiation of SCs, whereupon myelinating SCs downregulate expression of myelin-specific

View this article online at wileyonlinelibrary.com. DOI: 10.1002/glia.22572

Published online September 24, 2013 in Wiley Online Library (wileyonlinelibrary.com). Received Feb 4, 2013, Accepted for publication Aug 13, 2013.

Address correspondence to Jerold Chun, Molecular and Cellular Neuroscience Department, The Scripps Research Institute, 10550 North Torrey Pines Rd., DNC-118, La Jolla, CA 92037, USA. E-mail: jchun@scripps.edu

From the [1]Molecular and Cellular Neuroscience Department, Dorris Neuroscience Center, The Scripps Research Institute, La Jolla, California; [2]Department of Pharmacology, College of Pharmacy and Gachon Institute of Pharmaceutical Sciences, Gachon University, Incheon, Republic of Korea.

Brigitte Anliker, Ji Woong Choi, and Mu-En Lin contributed equally to this work.

proteins, re-express cell adhesion molecules and growth factors, and then proliferate (Jessen and Mirsky, 2008). Removal of LPA_1 in neuropathic pain models not only prevents the induction of neuropathic pain and demyelination, but also the down-regulation of myelin-associated proteins (Inoue et al., 2004; Lin et al., 2012; Nagai et al., 2010). These observations suggest that LPA/LPA_1 signaling mechanisms might impact normal myelination processes through induction of receptor subtype-mediated Schwann cell effects. By utilizing LPA_1-null mice, here we report that LPA/LPA_1 signaling promotes SC migration and contributes to normal SC-axon segregation and myelination.

Materials and Methods

G-Ratio Determination

Sciatic nerves were isolated from 13- to 26-week-old wild-type (WT) (*Lpar1*$^{+/+}$) and LPA_1 null mice (*Lpar1*$^{-/-}$). Generation of LPA_1 null mice by targeted disruption of exon 3 has been described previously (Contos et al., 2000). Sciatic nerves were fixed overnight in situ in freshly made 3% glutaraldehyde and 1% paraformaldehyde in 0.1 M sodium cacodylate buffer pH 7.4 containing 50 mM $CaCl_2$, and processed as described below. Semi-thin cross sections (1–2 μm) were stained with 0.1% toluidine blue for light microscopy. Image capture from the sections and measurement of the g-ratio was processed based on blinded determinations. Two image fields were taken from each nerve using a bright-field microscope equipped with a 100× oil objective lens and an AxioCam digital camera (Zeiss). For measuring the g-ratio, myelin thickness was determined using MetaMorph image analysis software (v6.3, Molecular Devices). Value of the g-ratio was obtained by dividing axonal diameter by total diameter (axon plus myelin, Fig. 1C) as described (Little and Heath, 1994).

Electron Microscopy

Sciatic nerves were removed after fixation from WT (*Lpar1*$^{+/+}$) and LPA_1 null mutant mice (*Lpar1*$^{-/-}$), contrasted with 1% osmium tetroxide in 0.12 M sodium cacodylate with 3.5% sucrose for 4 h at 4°C, washed, dehydrated through graded ethanol and acetone, and embedded in Epon/Araldite epoxy resin. Sections were made on a Leica Ultracut ultramicrotome for light and electron microscopy. The grids were contrasted with uranyl acetate and Reynold's lead citrate.

Primary Schwann Cell (SC) Culture

Murine SCs were isolated from dorsal root ganglia (DRG) at embryonic day (E) 13.5 as previously described (Kim, 1997). Isolated SCs were immunopositive for $p75^{NTR}$ (Chemicon), GFAP (Sigma), and S100 (Dako). The purity of the SCs was approximately >96% as assessed by cell size and morphology. After the first passage, SCs were cryoprotected in fetal bovine serum (FBS) with 10% DMSO and stored in liquid N_2. After thawing, cells were passaged on poly-L-lysine (PLL)-coated dishes for up to four passages. DMEM (Invitrogen) was supplemented with 10% FBS, 20 μg/mL pituitary extract (BD Biosciences), 2 μM forskolin (Sigma), and penicillin-streptomycin. Before migration and pull-down assays, SCs were serum-starved overnight in a modified "Sato" medium (Milner et al., 1997) consisting of DMEM (Invitrogen) complemented with 1× N2 supplement (Invitrogen), 20 μg/mL pituitary extract, 0.1 mg/mL fatty-acid free bovine serum albumin (FAFBSA, Sigma), 400 ng/mL of each T3 and T4 (Sigma), 4 μM forskolin, and penicillin-streptomycin. Receptor-deficient SCs and WT control cells from littermates were isolated from embryos at E13.5.

In Vitro Myelination

In vitro myelination was performed using E13.5 embryonic DRG neurons and SCs. In brief, DRGs were isolated from E13.5 WT embryos, digested with 0.25% trypsin for 40 min, triturated with a fire-polished Pasteur pipette into single cell suspension, and seeded onto PLL-Laminin coated cover slips in growth medium (DMEM with 10% FBS and 50 ng/mL NGF (Harlan)). Beginning the next day, the cells were treated with three cycles of antimitotic treatment, with 3 days in antimitotic medium containing 10 μM of both fluoro-deoxyuridine (FdU) and uridine (Sigma-Aldrich), and 2 days in conditioned growth medium. Two days after the antimitotic treatment, the medium was changed to serum-free conditions using DMEM/F12 medium (Invitrogen) containing 1× N2-supplement, 50 ng/mL NGF, and 2.5 μg/mL gentamycin (Invitrogen). The purified neurons were cultivated for 5 days to remove any residual FdU and uridine, before purified WT or LPA_1 null Schwann cells were added to the neuronal cultures. Myelination was induced 9 days later by adding 50 μg/mL ascorbic acid to the medium. The cultures were fixed with 4% PFA 2 weeks later and immunostained with an anti-MBP rat primary antibody (Serotec, 1:500) and a goat anti-rat AF568 secondary antibody (Molecular Probes, 1:500).

mRNA Expression Analysis Using Quantitative PCR

RNA was extracted from purified E13.5 DRG neurons and SCs using a TRIzol reagent (Life Technologies). To avoid genomic DNA contamination, extracted RNA was treated with DNase I. Reverse transcription was then performed using 1.5 μg RNA, oligo dT and GoScript reverse transcriptase (Promega). Quantitative PCR was performed on a Rotor-gene 3000 (Corbett Research) with GoTaq qPCR mix (Promega) with the following primer set: LPA_1 For: ATGGCAGCTGCCTCTACTTCC Rev: CCACCATGACCAGGA GATTGG, LPA_2 For: TCAGCCTAGTCAAGACGGTTG Rev: CATCTCGGCAGGAAT ATACCAC, LPA_3 For: ACACCAGTGG CTCCATCAG Rev: GTTCATGACGGAGTTG AGCAG, LPA_4 For: AGGCATGAGCACATTCTCTC Rev: CAACCTGGGTCTGA GAC TTG, LPA_5 For: AGGAAGAGCAACCGATCACAG Rev: ACC ACCATATGCAAACGA TGTG, LPA_6 For: GACAGCCCATCTCA CAATAC Rev: CGATAGGCAGTCGTTTAA GG, NRG1 Type III For: GCAAGTGCCCAAATGAGTTTAC Rev: GCTCCTCCGCTTC CATAAAT, ErbB2 For: CTCCATGATGGTGCTTACTC Rev: GTG TTGCGGTGAATG AGA, β-Actin For: TCGAATCCTGTGGCAT CCATGAAAC Rev: TAAAACGCAGCTC AGTAACAGTCCG.

Transwell Migration Assay

Cell migration was measured using transwells in a 24-well format (BD Bioscience) as previously described with minor modifications (Yamauchi et al., 2003). Briefly, 1.5 to 2.5 × 10^5 SCs in 300 μL

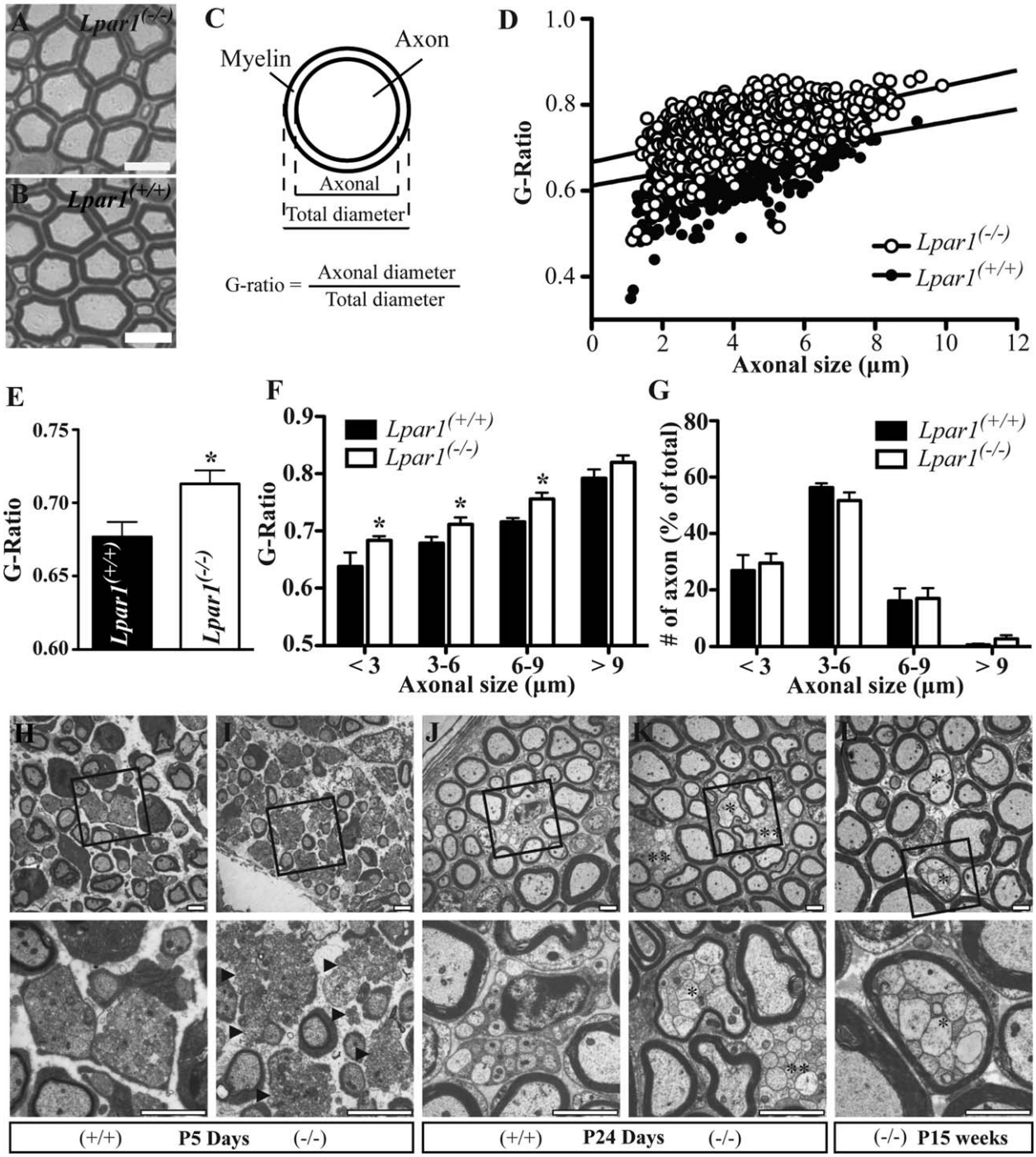

FIGURE 1: Deletion of LPA_1 in mice produces myelination and axonal segregation defects. **A–G**, Semi-thin cross sections (2 µm) of sciatic nerves from adult WT (*Lpar1*$^{(+/+)}$, $n = 5$) and LPA_1 null mice (*Lpar1*$^{(-/-)}$, $n = 7$) stained for myelin. Representative pictures of a sciatic nerve from adult LPA_1 null (**A**) and WT (**B**) mice are shown. **C**, Schematic diagram of g-ratio. **D**, G-ratio of individual fibers from two mice per group shown in a scatter plot. **E**, The mean g-ratio value was calculated from all nerves processed (mean ± SEM. * $P < 0.05$ *vs.* WT, *t*-test). **F**, Mean g-ratio values from all WT and LPA_1 null mice were calculated and grouped according to axonal diameter (means ± SEM * $P < 0.05$ *vs.* WT, *t*-test). **G**, The percentage of axons in sciatic nerves, as determined by axonal diameter, is equivalent in WT and LPA_1 null mice. **H–L**, Sciatic nerves from WT (**H**, **J**) and LPA_1 null (**I**, **K**, **L**) littermate mice were isolated at different ages and processed for electron microscopy. Representative pictures from sciatic nerves at postnatal day 5 (P5) (**H**, **I**), postnatal day 24 (P24) (**J**, **K**), and at 15 weeks of age (P15 weeks) are shown (**L**). Arrowheads indicate naked axon bundles (**I**); *polyaxonal myelination of small caliber axons (**K**, **L**); **axon bundles that are not ensheathed by SCs (**K**). (+/+) and (−/−) represent WT and LPA_1 null mice, respectively. Scale bars, 10 µm (**A**, **B**), 2 µm (**H–L**).

Sato medium was loaded onto collagen-coated polyethylene terephthalate transwell filters (8 μm pore size) and placed in wells containing 500 μL Sato medium. If cell-permeable inhibitors (50 μM LY294002, 100 nM Wortmannin, and 100 μM NSC23766) were used, cells were pretreated for 30 to 45 min before migration was induced. PTX was added to the cells overnight during serum-starvation at a concentration of 150 ng/mL. To induce directed SC migration across the membranes, LPA was added to the medium in the lower compartment at a final concentration of 500 nM unless otherwise indicated. After incubation at 37°C in 7.5% CO_2, the cells in the upper compartment were removed and migrated cells at the bottom side of the filters were stained with crystal violet and counted at six fields per filter. All experiments were done in triplicate and repeated two to four times.

For conditioned medium, murine DRGs at E13.5 were dissociated and plated at high densities in DMEM with 10% FBS and 50 ng/mL NGF (Harlan Bioproducts) onto PLL/laminin-coated glass coverslips. The next day, the medium was changed to serum-free conditions using DMEM/F12 medium (Invitrogen) containing 1× N2-supplement, 50 ng/mL NGF, and 2.5 μg/mL gentamycin (Invitrogen). To purify DRG neurons, three cycles of anti-mitotic treatment using 10 μM FdU (Sigma) and 10 μM uridine (Sigma) were performed. Conditioned medium was collected 5 days after the last medium change. Alternatively, anti-mitotic treatment was omitted to collect conditioned medium from SC/neuron co-cultures. Conditioned medium was subsequently used as a chemoattractant in the lower compartments of transwells for SCs plated in DMEM/F12 medium supplemented with N2, NGF, and gentamycin onto the filters.

Migration Assay Along Axon Bundles

Induction of SC migration along axon bundles of cultured DRG neurons was performed as described (Yamauchi et al., 2004). Briefly, murine WT DRGs were isolated and neurons were grown in parallel lanes along collagen stripes on glass coverslips. During anti-mitotic treatments DRG neurites became fasciculated. GFP-expressing transgenic mice (Okabe et al., 1997) were crossed into the LPA_1 null and wildtype background, from which GFP-expressing SCs were isolated. GFP-expressing WT and LPA_1 null SCs were reaggregated overnight on a non-permissive substrate with constant agitation. The next day, SC aggregates were plated onto the bundled WT DRG neurites, and migration of SCs away from the aggregates and along the neurites was examined either in the presence or absence of 1 μM LPA. After 6 to 7 h, the cultures were fixed and immunostained for neurofilaments (αNF-200, Serotec). Nuclei were stained with DAPI and images were acquired using a fluorescence microscope fitted with an AxioCam camera (Carl Zeiss, Thornwood, NY). Migration of all SCs detached from individual aggregates was determined by measuring the distance from the single SC nuclei to the periphery of the aggregates.

LPA Measurement in the Conditioned Medium

All extraction processes were done using 1.5 mL low adhesion tubes (Fisher Scientific) and low adhesion pipette tips (Axygen) on ice to prevent LPA loss. In all samples, 1 μM of C17 LPA (Avanti Polar Lipids) was added immediately before extraction as an internal standard. Conditioned medium (1 mL/sample) was collected. The same volume of MeOH-HCl 10:1 mix and a half volume of chloroform were added sequentially and vortexed. The mixture was then incubated on ice for 40 min. Saturated NaCl in water (280 μL) was added and mixed gently by inverting the tube. After 10 min, the bottom phase (organic phase) was collected after centrifugation at 14,000 rpm at 4°C. Samples were dried down using a Vacufuge (Eppendorf) and reconstituted with 50 μL of methanol.

Mass spectrometry (MS) analysis was done in TSRI's Mass Spectrometry Core using an Agilent 6410 triple quad mass spectrometer coupled to an Agilent 1200lc stack for high performance liquid chromatography (HPLC). An extended C18 column with a 21 × 150 mm dimension, 3.5 μm particle size, and 150 μL/min flow rate was used for reverse phase separation of the extracted sample. The reverse phase separation was performed with the following solvent conditions: Solvent A = 95:5 H_2O:MeOH 0.1% NH_4OH, B = 60:35:5 IPA:MeOH:H_2O 0.1% NH_4OH. Mobile phase starting with 50:50 = A:B for 3 min and ramped up to 100% B in 10 min. Eluent was analyzed with the following parameters for 18:1 LPA: (*m/z*: 435 →153 and 435→79) and 17:0 LPA (*m/z*: 423→153 and 423→79). Negative ion mode was used as follows: Fragmentor voltage = 160 V, collision energy = 20 V, drying gas flow rate = 10 L/min, temp = 35°C, nebulizer pressure = 30 psi, and capillary voltage = 4,500 V.

Rac Pulldown Assay

The PBD pulldown assay for measuring Rac GTPase activation, including the expression and purification of the GST-PAK1 PBD fusion protein, has been described in detail elsewhere (Benard and Bokoch, 2002). Briefly, SC cultures were serum-starved overnight in Sato medium. Cells were stimulated with 1 μM LPA for the indicated times. Cells were washed twice with ice-cold PBS and lysed in 800 μL ice-cold lysis buffer (25 mM Tris buffer, pH 7.5, 40 mM NaCl, 30 mM $MgCl_2$, 1 mM DTT, 0.5% NP-40, 1 mM PMSF, 10 μg/mL leupeptin, 10 μg/mL aprotinin). Cell lysates were cleared by centrifugation at 14,000 rpm for 10 min at 4°C. Cleared lysates (10 μL) were used for total protein control. The remaining lysates were incubated with 20 to 30 μg GST-PAK1 PBD beads for 1 h at 4°C. Subsequently, the beads were washed 4× with 0.5 mL lysis buffer before bound Rac was eluted from the beads and analyzed by standard SDS-PAGE and Western blotting techniques using a monoclonal anti-Rac1 antibody (Upstate Biotechnology). Film images were scanned for densitometric analysis.

Results

LPA_1 Deficiency Increases the G-Ratio in Sciatic Nerves

To identify whether LPA_1-mediated signaling alters myelination, sciatic nerves were isolated from LPA_1 null mice (*Lpar1*$^{-/-}$) and wild-type littermate controls (WT, *Lpar1*$^{+/+}$) and processed for ultrastructural analyses. The g-ratio (axon diameter divided by fiber diameter), which reports thickness of the myelin sheath in relation to the axon diameter, was determined and compared between adult LPA_1 null mice ($n = 7$) and WT controls ($n = 5$). Decreased myelin thickness was observed in sciatic nerves from LPA_1 null mice when compared with sciatic

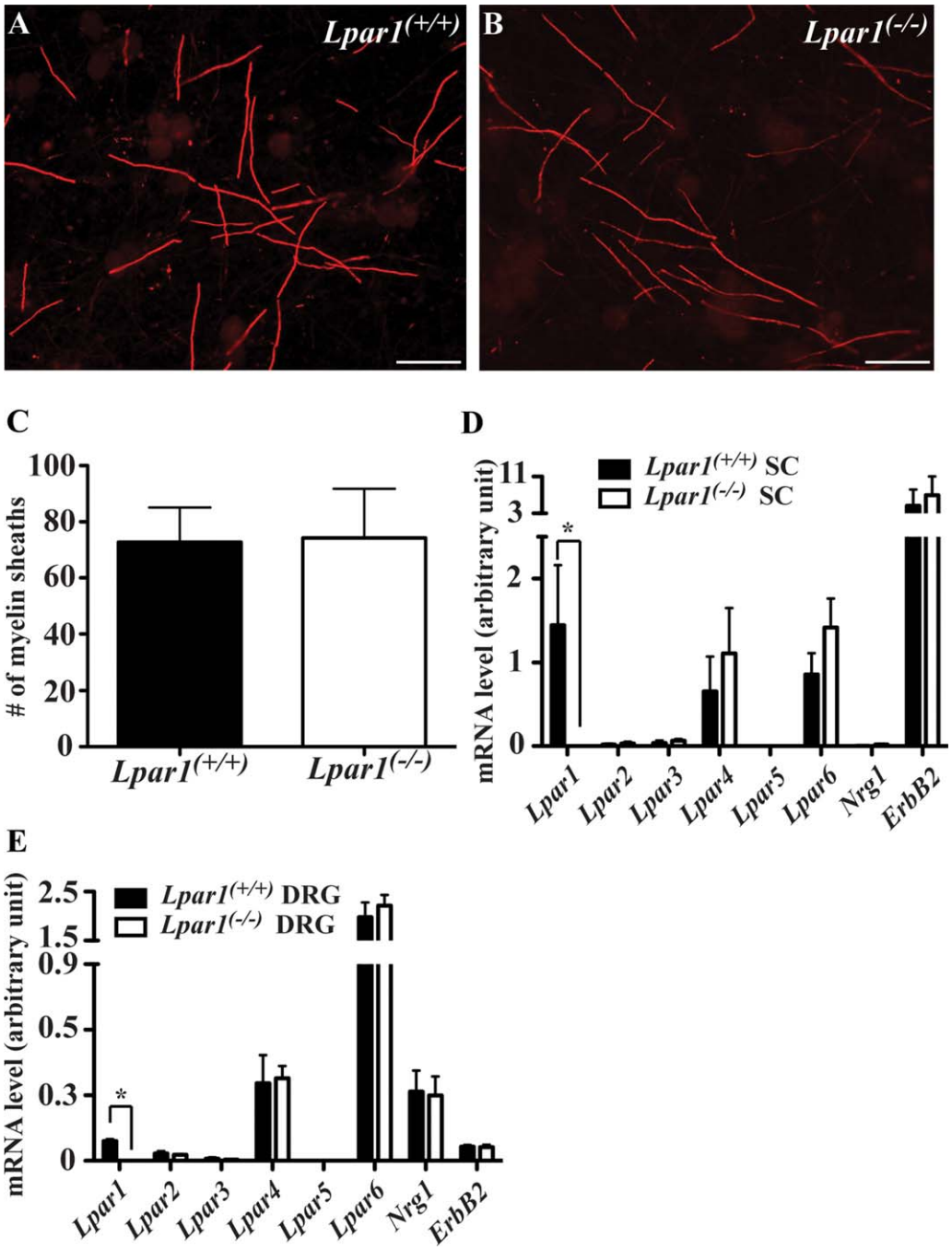

FIGURE 2: Myelination capability and expression levels of other LPA receptors are not affected in LPA_1 null Schwann cells. A-C, ***In vitro*** **myelination analysis using purified E13.5 Schwann cells and DRG neurons. WT (A) and LPA_1 null (B) SCs were added to purified WT DRG neurons and myelination was induced by addition of ascorbic acid for 2 weeks. Myelin sheaths were visualized by immunostaining using an antibody against myelin basic protein (MBP). Scale bar, 100 μm (A, B). MBP positive segments were quantified at five fields per coverslip. (Mean ± SD, $n = 4$). (C). D, E, mRNA expression levels of LPA_{1-6}, NRG1 Type III, and ErbB2 in purified E13.5 SC (D) and DRG neurons (E) were examined using qPCR (normalized to β-Actin, $n = 3$, mean ± SD, * $P < 0.05$, *t*-test). [Color figure can be viewed in the online issue, which is available at wileyonlinelibrary.com.]**

nerves from WT mice (Fig. 1A–F), resulting in a statistically significant increase in the mean g-ratio from 0.677 ± 0.010 in WT controls to 0.713 ± 0.009 in LPA_1 null mice (Fig. 1D). This difference was not accompanied by changes in axonal size, since the percentages of axons with a given axonal diameter were similar between LPA_1 null mice and WT controls (Fig. 1G).

Reduced Axonal Segregation and Polyaxonal Myelination in LPA_1 Null Mice

Transmission electron microscopic analysis of sciatic nerves from LPA_1 null mice of different ages (postnatal day 5 to 15 weeks old) revealed signs of defective axonal segregation (Fig. 1H–L). In nerves from 5-day-old (P5) LPA_1 null mice, axonal

segregation of small caliber axons appeared to be delayed compared with WT controls. In the absence of LPA_1, SCs were still able to establish a 1:1 relationship with large caliber axons, however, many of the small caliber axon bundles lacked interacting SCs (Fig. 1I, arrowhead). In contrast, nerves from WT mice, showed ensheathment of the small caliber axons and the formation of Remak bundles (Fig. 1H). By postnatal day 24 (P24), formation of Remak bundles in WT mice was complete (Fig. 1J), whereas in LPA_1-deficient mice, naked small caliber axons were still frequently observed (Fig. 1K, double asterisk). Naked axons were not observed in adult mice indicating that the ensheathment of small caliber axons and the formation of Remak bundles is delayed in LPA_1 null mice but not abolished (data not shown). Notably, by P24, an increased incidence of polyaxonal myelination identified by bundles of small caliber axons enveloped by a single thin myelin sheath was evident in LPA_1-null mice (Fig. 1K, asterisk). It has been reported that polyaxonal myelination can occasionally occur in young WT mice during active myelination but is corrected with further development (Rasi et al., 2010). However, in adult LPA_1-null mice, bundles of small caliber axons wrapped by a single myelin sheath were still present (Fig. 1L, asterisks) through 57 weeks of age (data not shown). No polyaxonal myelination was observed in adult WT littermates. Overall, these analyses of sciatic nerves from LPA_1-null mice identify requisite roles for LPA_1 in regulating the normal segregation of small-caliber axons and in establishing the appropriate thickness of the myelin sheath.

Myelination Capability In Vitro is Not Affected in LPA_1 Null Schwann Cells

In order to determine whether the myelination capability of SCs is affected by the removal of LPA_1, we utilized an *in vitro* myelination system using purified DRG neurons and SCs. WT or LPA_1 null SCs were allowed to myelinate purified WT DRG neurons *in vitro* (Fig. 2A, B). No significant differences in the number and length of myelin segments were observed (Fig. 2C, data not shown). This demonstrates that the basic myelination machinery is not affected by the removal of LPA_1 in SCs.

In order to rule out the possibility of compensatory upregulation of other LPA receptors or NRG, we examined mRNA expression levels using qPCR in both purified SCs and DRG neurons. No significant alteration of LPA_{2-6}, NRG, or ErbB2 mRNA expression levels were observed (Fig. 2D, E) suggesting that the consequences of LPA_1 deficiency are not masked by upregulation of other known LPA receptors or altered expression levels of NRG and ErbB2 in LPA_1-null mice.

LPA Enhances SC Migration in a Dose-Dependent Manner Through LPA_1

The delay in axonal segregation observed in LPA_1 null mice could involve defects in SC migration. In order to determine if LPA could influence SC migration, LPA-dependent migratory responses of primary mouse SCs derived from WT mice were assessed with a transwell chamber assay. LPA strongly induced SC migration in a dose-dependent manner (Fig. 3A, B). LPA at a concentration as low as 10 nM induced SC migration indicating that this response was receptor-mediated. Indeed, primary SCs isolated from newborn mice and rats are known to express a variety of LPA receptors (Li et al., 2003; Weiner and Chun, 1999; Weiner et al., 2001), and data from RT-PCR analysis demonstrated that cultured embryonic mouse SCs express $LPA_{1,4,6}$, and to a lesser extent, the $LPA_{2,3}$ receptors (Fig. 2D). In order to identify which LPA receptor subtypes mediated the LPA dependent SC migratory responses, we isolated SCs from LPA_1 (*Lpar1*$^{-/-}$), LPA_2 (*Lpar2*$^{-/-}$), and LPA_3 (*Lpar3*$^{-/-}$) null mice and compared their migratory responses towards LPA. SCs deficient for LPA_2 or LPA_3 showed LPA-dependent migratory responses similar to WT SCs (Fig. 3C). However, a virtually complete loss of LPA-induced migration was observed in LPA_1 null SCs (Fig. 3C). To assure the basic migration capability was not generally impaired in LPA_1-deficient SCs, the migratory response to sphingosine 1-phosphate (S1P) (500 nM), another lysophospholipid that acts upon related GPCRs, was examined. Similar to WT SCs, LPA_1 null SCs revealed a 2–3 fold increase in migration upon stimulation with S1P (data not shown). The capability of S1P to induce migration of LPA_1-deficient SCs indicates that G protein-mediated migratory pathways are intact, supporting an LPA_1 specific migration defect in LPA_1 null SCs.

LPA Released by DRG Neurons Mediates SC Migration

LPA_1-dependent SC migration would require an endogenous source of LPA to be physiologically relevant. In view of their proximity to developing SCs, and prior data from the cerebral cortex indicating the developmental production of LPA by postmitotic neurons (Fukushima et al., 2000), DRG neurons are one potential source of LPA. In support of this LPA source, conditioned media from purified and unpurified mouse DRG neurons in culture were analyzed by HPLC-MS and found to have LPA present at concentrations of 3.322 ± 0.158 and 2.345 ± 0.237 nM, respectively (Fig. 3D), values that approximate the EC_{50} of LPA_1 (Hecht et al., 1996).

To examine whether LPA produced by DRG neurons can promote SC migration, we used conditioned media from DRG neurons in culture as a migration stimulus in the transwell assay. Conditioned media from either murine DRG neurons/SC co-cultures (unpurified) or purified DRG neurons markedly enhanced WT SC migration (Fig. 3E, F). We subsequently compared the capability of WT and LPA_1 null SCs

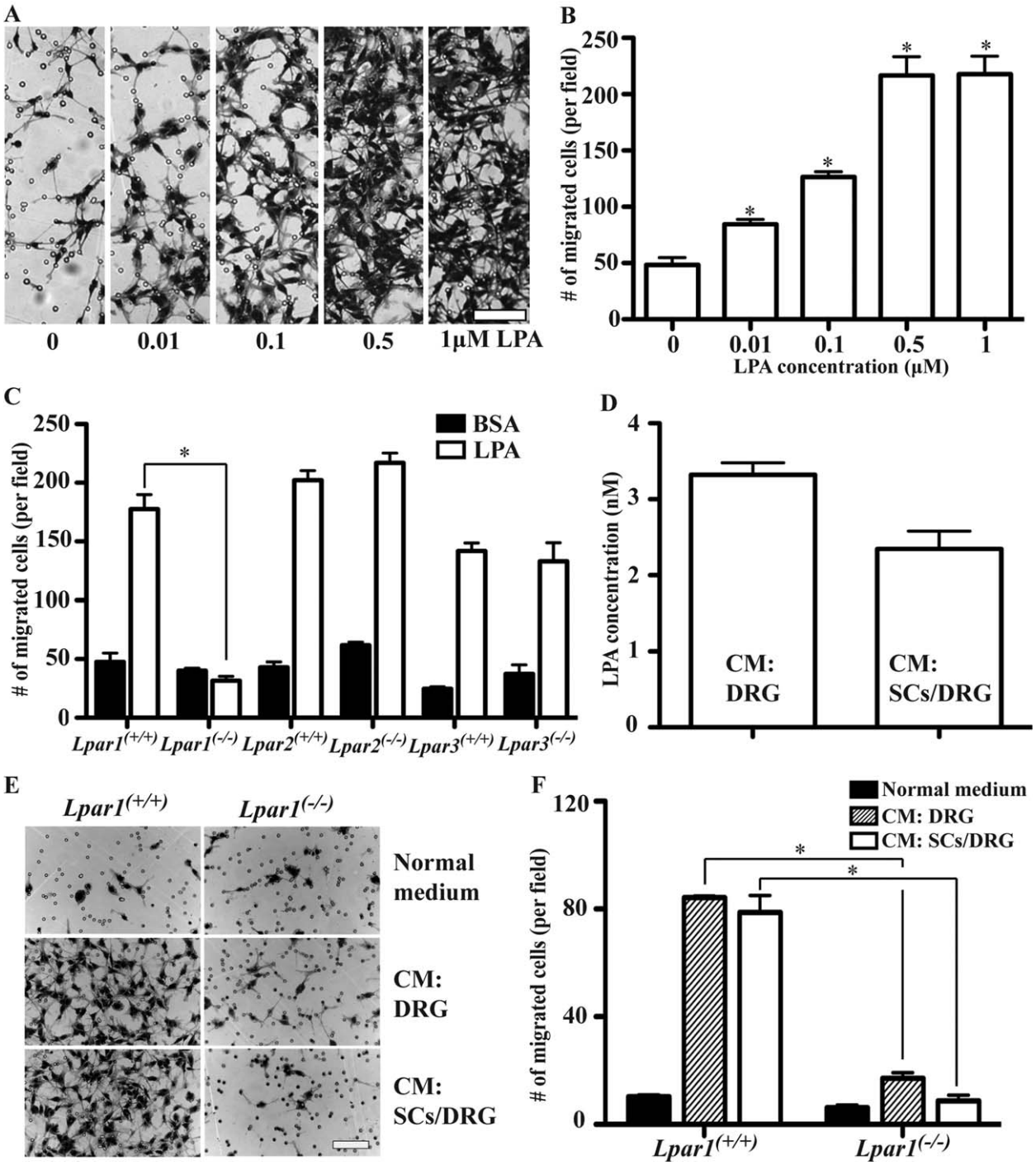

FIGURE 3: LPA produced by neuronal cells mediates SC migration through LPA_1. **A, B,** Increasing concentrations of LPA added to the lower compartments of transwell chambers induced SC migration across a membrane with an 8 μm pore size. SCs that migrated to the bottom side of the membrane after 5 to 6 h were stained with crystal violet (**A**) and quantified (**B**). Shown are mean ± SEM. ($n = 5$, $*P < 0.05$ *vs.* control (0.1% BSA), *t*-test) (**B**). **C,** Comparison of migration of WT and $LPA_{1/2/3}$ null SCs toward LPA. Mean ± SEM of one representative example of four independent experiments ($n = 3$, $*P < 0.05$ *vs.* basal migration under control conditions, *t*-test). **D,** LPA concentration in the conditioned medium from purified DRG neurons (CM: DRG) or DRG neuron/SC co-cultures (CM: SCs/DRG) as measured by HPLC/MS. mean ± SEM ($n = 6$). **E, F,** Transwell migration of WT and LPA_1 null SCs in response to control or conditioned media from purified DRG neurons (CM: DRG) or DRG neuron/SC co-cultures (CM: SCs/DRG). Representative photographs are shown after 5 to 6 h of migration (**E**), the number of SCs that migrated to the bottom side of the transwells was quantified (**F**). Mean ± SEM of a representative example of four independent experiments ($n = 3$, $*P < 0.05$ *vs.* same treatment in WT group, *t*-test). Scale bar, 100 μm (**A, E**).

with migrate in response to the endogenous LPA present in the conditioned media. Media from neurons/SC co-cultures or from purified neurons enhanced migration of WT SCs 5- to 6.5-fold over controls (Fig. 3E, F). However, in the absence of LPA_1, SC migratory responses to conditioned media from DRG neuron cultures were greatly reduced: LPA_1-deficient SCs showed a 65 to 70% reduction in migration compared with WT SCs (Fig. 3E, F). These observations demonstrated that extracellular LPA is produced by DRG neurons and this source of LPA is a potent inducer of SC migration through LPA_1.

SC Migration Along DRG Neurites

To further assess the physiological relevance of LPA-induced SC migration beyond the transwell assay, we assayed SC migration along purified WT mouse DRG axons in culture (Fig. 4). GFP-labeled WT or LPA_1-null SC aggregates were seeded onto DRG axons, and allowed to migrate out from the aggregates for 6 to 7 h either in the presence or absence of exogenous LPA. Consistent with the DRG production of LPA, WT SCs exposed to control medium still migrated away from the SC aggregates while LPA_1-null SCs showed less migration. The addition of 1 μM LPA to the control media significantly increased the average migration distance of WT SCs by approximately 20% (Fig. 4D, E, F, M), but did not enhance migration of LPA_1-null SCs, demonstrating LPA_1-dependent SC migration on intact axons (Fig. 4J, K, L, M). In the absence of exogenous LPA, the average migration distance of LPA_1-null SCs (Fig. 4G, H, I, M) was reduced by about 27% as compared with migration distance observed with WT SCs (Fig. 4A, B, C, M). These results identify LPA_1-dependent SC migration along DRG axons. In addition, they also identify endogenous LPA effects, manifested by WT SC migration in control medium, which is reduced upon LPA_1 removal, while also implicating LPA independent migration mechanisms, as expected, by virtue of basal SC migration that is independent of LPA_1 genotype (Fig. 4M).

LPA_1 Enhances SC Migration Through G_i Proteins and the Small GTPase Rac

LPA_1 is known to couple to three heterotrimeric G protein complexes, as defined primarily by their alpha subunits G_i, G_q, and $G_{12/13}$, thereby linking the receptor to multiple downstream signaling pathways (Choi et al., 2010). To determine which signaling pathways were involved in mediating the LPA-induced migration response, downstream pathway inhibitors were used in the SC transwell migration assay. Treatment of WT SCs with either pertussis toxin (PTX, Fig. 5A), a specific inhibitor for G_i proteins, or NSC23766 (Fig. 5B), an inhibitor of the small GTPase Rac1, completely abolished LPA-induced SC migration. Blocking of phosphoinositol 3 kinase (PI3K), that mediates signaling between G_i and Rac1, by administration of the PI3K inhibitor LY294002, only marginally reduced LPA-induced SC migration (Fig. 5C). The average fold induction of LPA-induced SC migration over four independent experiments was reduced from 3.16-fold to 2.51-fold in the presence of 50μM LY294002 ($P = 0.0157$), while basal cell migration was markedly reduced (data not shown). The less selective compound wortmannin also reduced basal SC migration, while the small effects on the induction of LPA-mediated SC migration observed with LY294002 were not detected with wortmannin exposure. To verify activation of Rac1 through LPA_1, we measured the activation state of endogenous Rac1 using a GST-PBD pull-down assay. In WT SCs, LPA enhanced Rac1 activation in a time-dependent manner (Fig. 5D). Maximum levels of activated Rac1 were obtained at 30 min following stimulation with LPA and the elevated levels of activated Rac1 persisted for at least 90 min after stimulation (not shown). We typically observed a two to threefold increase in GTP-bound Rac1 compared with non-stimulated cells. In contrast to WT SCs, no Rac1 activation was observed in LPA_1-deficient SCs after stimulation with LPA (Fig. 5D). These results indicate that LPA-induced Rac1 activation through LPA_1 is a major component of SC migration.

Inhibitors of additional key migratory molecules, including the mitogen-activated protein kinases (MAPKs), Erk1/2, p38, and JNK, (Fig. 5E, F), or the small GTPase Rho, and its associated kinase ROCK (Fig. 5F), only partially reduced overall SC migration without specifically blocking LPA-induced migration. This was demonstrated by the use of inhibitors PD98059 (Erk inhibitor), SB203580 (p38 inhibitor), SP600125 (JNK inhibitor), and Y27632 (ROCK inhibitor). Overall, these observations identified G_i and Rac1, as the primary mediators of LPA-induced SC migration through LPA_1.

Discussion

This study identifies a novel role for the bioactive lipid LPA and one of its six receptors, LPA_1, in SC migration and peripheral nerve development. It identifies LPA_1/G_i/Rac1 as the major signaling pathway responsible for inducing chemotactic SC migration towards LPA that can be secreted by DRG neurons (Fig. 6). Disruption of LPA_1 signaling is associated with adult sequelae within peripheral nerves, consisting of polyaxonal ensheathment and reduced thickness of myelin sheaths *in vivo*.

Migration of SC precursors along outgrowing axons precedes other important cellular processes, such as axonal segregation of small caliber axons and radial sorting of large diameter axons, which are required for SC differentiation to either nonmyelinating or myelinating cells (Jessen and Mirsky, 2005; Voyvodic, 1989). Thus, impaired or delayed SC migration could

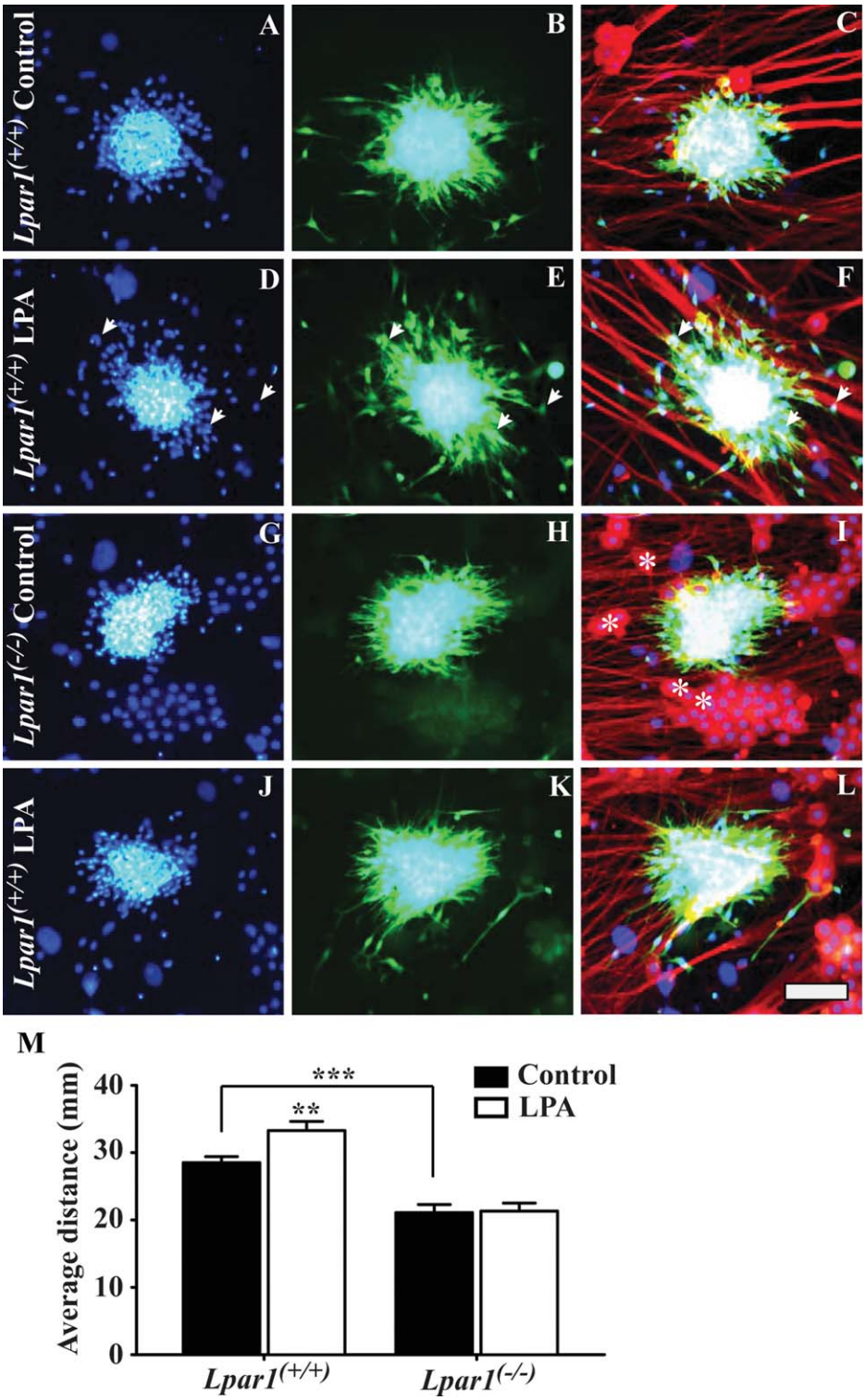

FIGURE 4: LPA induces SC migration along purified DRG neurons through LPA_1. **A–L**, Aggregated WT (**A–F**) or LPA_1-null SCs (**G–L**) expressing a GFP transgene were added to purified DRG neuronal cultures and incubated in the presence of vehicle (0.1% BSA, **A**, **B**, **C**, **G**, **H**, **I**) or 1 μM LPA (**D**, **E**, **F**, **J**, **K**, **L**) for 6 to 7 h. DAPI staining shows the nuclei of SCs and neurons (**A**, **D**, **G**, **J**). In addition, SCs were detected via GFP fluorescence (**B**, **E**, **H**, **K**), and DRG neurons were stained for neurofilaments to visualize axons (red in **C**, **F**, **I**, **L**). Merged images are also shown (**C**, **F**, **I**, **L**). Some of the neuronal cell soma are indicated with asterisks (**I**). Scale bar, 100 μm. **M**, LPA-induced migration from the aggregates along the fasciculated DRG axons was quantified by measuring the average distance of migrated SCs from the periphery of the aggregates. (Arrowhead, **D**, **E**, **F**) Mean ± SEM of a representative example of three independent experiments ($n = 8$, $^{**}P = 0.0028$, $^{***}P = 0.0003$, *vs.* migration of WT cells under control conditions, *t*-test).

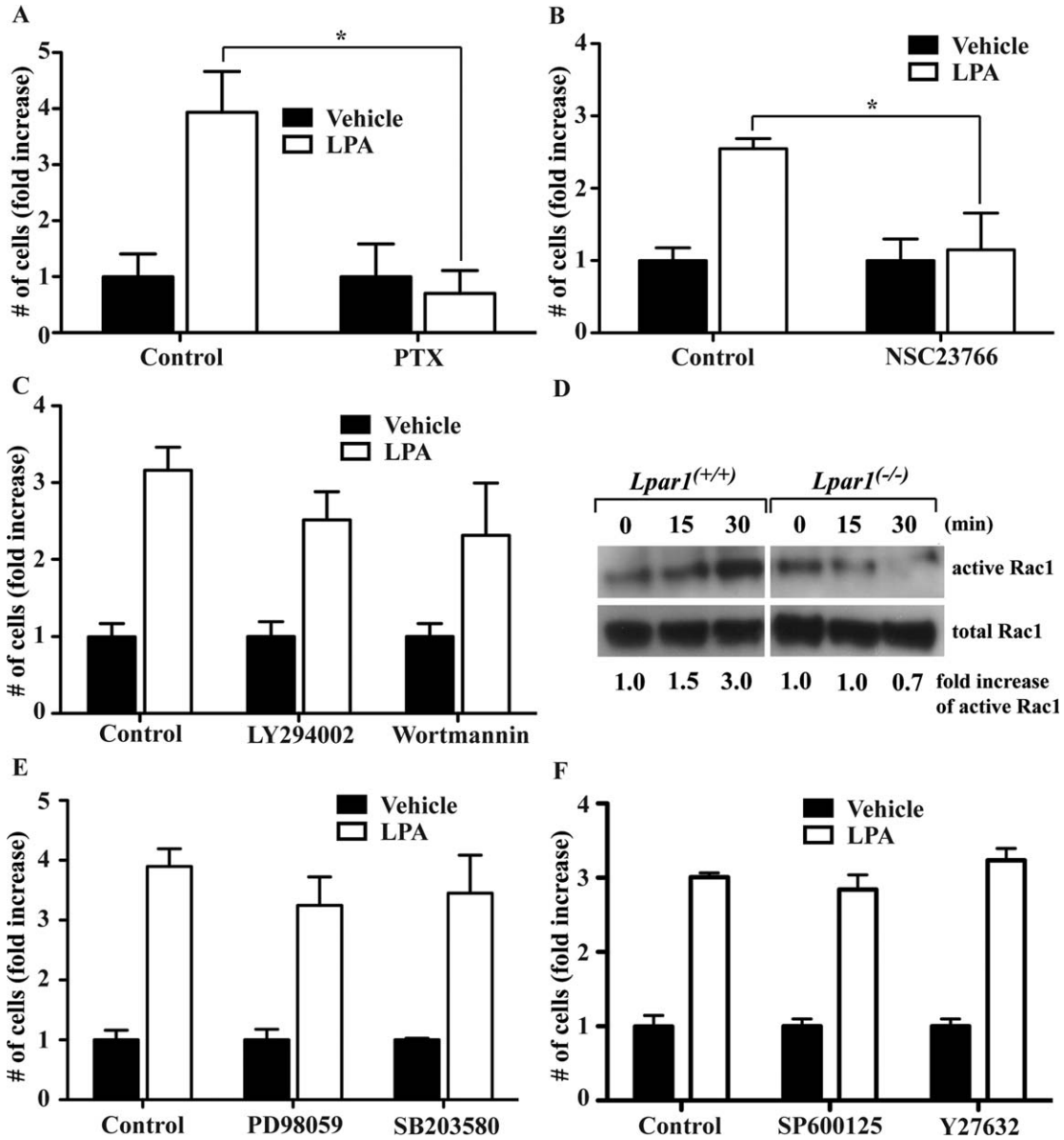

FIGURE 5: G_i proteins and the small GTPase Rac1 are involved in LPA/LPA_1 signaling-mediated SC migration. **A–C**, WT SCs were pretreated overnight with 150 ng/mL pertussis toxin to inhibit G_i proteins (**A**), or treated for 30 to 45 min with either 100 μM NSC23766 to block Rac1 (**B**) or 50 μM LY294002 and 100 nM wortmannin to inhibit PI3K (**C**) before SC migration was induced by adding 500 nM LPA to the lower transwell compartment. After 5 to 6 h, LPA-induced migration was quantified and compared with the vehicle (0.1% BSA)-induced migration of SCs treated with the respective inhibitors and to the responses of untreated SCs (**A–C**). Fold-increased over vehicle treated cells are presented as mean ± SD of representative examples of two to four independent experiments ($n = 3$, $^*P < 0.05$, *t*-test). **D**, Activation of endogenous Rac1 upon treatment with 1 μM LPA in WT or LPA_1 null SCs. GTP-bound Rac1 was pulled down from cell lysates at the indicated time points after addition of 1 μM LPA using a GST-tagged PAK-binding domain. Active GTP-bound and total Rac1 levels were subsequently analyzed by Western blotting. The fold increase of activated Rac1 at the different time points was measured and normalized against the total Rac1 levels. Shown are representative examples of two to three independent experiments. The involvement of MAPKs including ERK1/2, p38, JNKs, and the Rho kinase ROCK was determined using specific inhibitors for each protein. WT SCs were pretreated for 30 min with 50 μM PD98059 (**E**), 20 μM SB203580 (**E**), 10 μM SP600129 (**F**), or 10 μM Y27632 (**F**) to inhibit the activation of ERK1/2, p38, JNKs, or ROCK before migration was induced by adding 500 nM LPA to the lower transwell compartments. Values represent mean ± SD of representative examples of two independent experiments (**E**, **F**).

contribute to the large amount of naked or insufficiently enveloped small caliber axon bundles detected in the sciatic nerves of LPA_1 null mice at P5. During further development, the naked bundles of small caliber axons became ensheathed by SCs, indicating that the reduced axonal segregation observed at P5 is due to delayed, rather than defective, axonal segregation.

Additional alterations observed in peripheral nerves of adult LPA_1 null mice included a reduced thickness in myelin

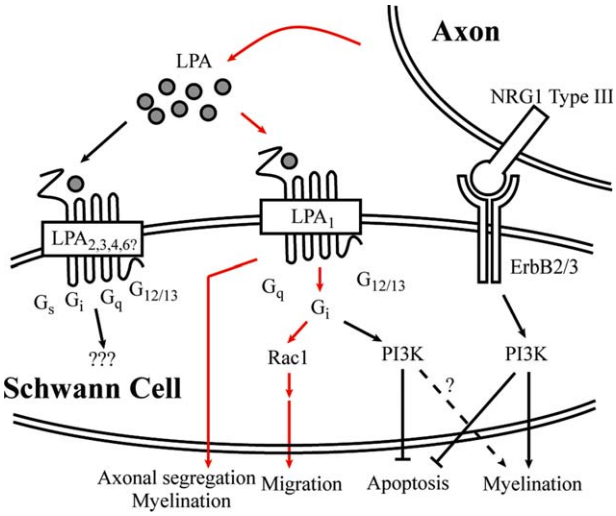

FIGURE 6: Schematic model of LPA/LPA_1 signaling in SCs and its effects on SC developmental processes. LPA secreted by DRG neurons increases SC migration through binding to LPA_1 and subsequent activation of G_i proteins and the small GTPase Rac1. Removal of LPA_1 *in vivo* results in delayed axonal segregation and aberrant myelination suggesting that LPA/LPA_1 signaling either directly or indirectly modulates axonal segregation and myelination. Since binding of LPA and NRG to their receptors LPA_1 and ErbB2/ErbB3 can activate similar downstream signaling pathways, as shown for the previously described anti-apoptotic effect in SCs, it is possible that LPA_1 modulates activation of downstream effectors of the NRG/ErbB2/ErbB signaling pathways regulating axonal segregation and myelination. Whether other LPA receptors ($LPA_{2,3,4,6}$) expressed in SC are involved in SC differentiation processes has not been clarified. [Color figure can be viewed in the online issue, which is available at wileyonlinelibrary.com.]

sheaths and an increased incidence of polyaxonal myelination of small caliber axon bundles suggesting a mild but distinct effect of LPA_1 in axonal segregation and myelination. Type III β1a neuregulin (NRGβ1a type III) is the key myelination trigger, which determines whether axons are ensheathed or myelinated, and also governs myelin sheath thickness (Michailov et al., 2004; Taveggia et al., 2005). Low axonal NRG type III expression results in an ensheathing phenotype, while high axonal expression induces the formation of a myelin sheath. In addition, NRGβ1a type III is also required for proper segregation and ensheathment of small caliber axons by SCs (Taveggia et al., 2005). Interestingly, overexpression of the second known NRG type III isoform, NRGβ3 type III, also revealed profound effects on Remak bundles, as the small caliber axons of the bundles were closely packed and no longer segregated from one another by SC cytoplasm (Gomez-Sanchez et al., 2009), with a significant number of these bundles myelinated as a single unit, as was observed in the LPA_1 null mice. The similarities between the consequences of deregulated NRG type III and LPA/LPA_1 signaling suggest overlapping activities in myelination, a result that is consistent with LPA/LPA_1 and NRG signaling previously reported for SC survival (Weiner and Chun, 1999). Although LPA and NRG bind to different receptor classes (NRG type III isoforms binding to ErbB receptor tyrosine kinases and LPA to GPCRs), they are nonetheless able to activate similar downstream signaling pathways, as shown for SC survival. Both NRG and LPA prevented SC apoptosis through activation of PI3K and Akt (Li et al., 2001; Weiner and Chun, 1999). Moreover, NRG is able to activate RAS-MAPK pathways in SCs (Taveggia et al., 2005), which can also be activated through LPA_1 (Anliker and Chun, 2004). We hypothesize that LPA/LPA_1 signaling might to some extent modulate the activation state of the downstream effectors of the dominant NRG/ErbB signaling pathways in SCs during phases of axonal segregation and myelination, thus representing a lipid modulator of NRG activities. While expression levels of NRG1 TYPE III and ErbB2 are not affected by the loss of LPA_1 in either DRG neurons or SCs as shown by qPCR analysis, it remains to be determined whether LPA_1 and NRG signaling converge in regulating myelination.

While these considerations imply an important role of LPA_1 in SCs, we cannot exclude a role of neuronal LPA_1 in reducing myelin thickness and increasing incidence of polyaxonal myelination of small caliber axon bundles. Conditional LPA_1 null mice are needed to reliably identify the neuronal or SC LPA_1 contribution to the observed phenotype. Also, the role of LPA_1-induced Rac1 activation in myelinating SCs remains to be elucidated. Rac1 has been reported to be essential for the myelination process, since SC process extension and stabilization, as well as radial sorting of axon bundles, requires activation of Rac1 by β1 integrins (Benninger et al., 2007; Nodari et al., 2007). The *in vitro* myelination assay, however, revealed that LPA_1 null SCs were still capable of extending processes, enwrapping the axons and forming myelin sheaths. Nevertheless, we cannot exclude the possibility that differentiating LPA_1 null SCs have lower levels of active Rac1 through the loss of LPA_1, which might contribute to some of the defects observed in the sciatic nerves of LPA_1 null mice.

Several ligands including NRG, NT3, and nerve growth factor (NGF) that were shown to induce SC chemotaxis *in vitro*, could potentially be involved in the regulation of developmental processes associated with SC movements (Anton et al., 1994; Jessen and Mirsky, 2005; Mahanthappa et al., 1996; Meintanis et al., 2001; Yamauchi et al., 2003). The present study identifies LPA as another strong candidate for regulating SC movements *in vivo*, since LPA appears to be a dominant pro-migratory factor released from DRG neurons *in vitro*. Using conditioned medium from DRG neurons, we observed a 65 to 75% reduction in the migratory response of LPA_1-deficient SCs compared with WT cells. The remaining induction of SC migration in LPA_1-deficient cells was marginally due to S1P, as observed by comparison with SCs

deficient for both LPA_1 and $S1P_3$, the receptor mediating S1P-induced SC migration (unpublished data) (Mutoh et al., 2012). Thus, only 20–25% of the increase in SC migration by conditioned media was independent of lysophospholipid signaling mechanisms *in vitro*.

This observation is particularly striking in view of the lack of SCs along peripheral nerves in NRG type III-, ErbB2-, and ErbB3-deficient mice or zebrafish (Garratt et al., 2000; Lyons et al., 2005). In zebrafish, NRG signaling through ErbB2/ErbB3 receptor tyrosine kinases exhibited an essential role for directed SC migration along axon bundles (Lyons et al., 2005). In mice, NRG did not reveal a pro-migratory effect when E12.5 WT DRGs were used for studying SC migration out of the ganglia (Morris et al., 1999), with modest NRG-induced migration observed when DRGs from newborn mice or rats were used (Mahanthappa et al., 1996; Morris et al., 1999; Woldeyesus et al., 1999). This latter observation suggests that NRG is capable of inducing SC migration of neonatal mouse SCs, but not of embryonic SC precursors isolated at E12.5, while documented species differences in lysophospholipid receptor roles between Zebrafish and mice (Ishii et al., 2002; Kupperman et al., 2000) may contribute to the different SC outcomes. Species differences and developmental stages may also account for dominant LPA_1 SC effects observed here: prior studies identifying NRG as the key inducer of SC migration present in conditioned medium from DRG neurons (Yamauchi et al., 2008) used SCs isolated from rat neonates rather than the embryonic SCs from E13.5 mouse DRGs utilized here. A change in the responsiveness to pro-migratory stimuli of differentiating SCs could provide an explanation for the minor phenotype observed in LPA_1 null mice, wherein NRG or other signaling molecules might induce SC migration at later embryonic or perinatal developmental stages to ultimately compensate for the loss of LPA_1.

While the underlying signaling mechanisms for SC survival are comparable for LPA and NRG, the migratory response seems to be differentially regulated (Li et al., 2001; Meintanis et al., 2001; Weiner and Chun, 1999). Migration in response to NRG was partially mediated by MAPKs and PI3Ks (Meintanis et al., 2001). In contrast, LPA-induced migration was at best only marginally blocked by MAPK or PI3K inhibitors. The latter result was unexpected since it is well known that the $\beta\gamma$-subunits of G_i proteins activate PI3Ks, whose phosphoinositide products subsequently activate Rac-GEFs, such as Tiam1 or P-Rex-2b (Li et al., 2005; Van Leeuwen et al., 2003). Furthermore, in glioma cells, LPA was found to induce migration partially through the LPA_1/G_i/PI3K/Rac/JNK signaling pathway (Malchinkhuu et al., 2005). It is possible that the pathway mediating cell migration in SCs is different than the one observed in glioma cells. On the other hand, we cannot exclude the possibility that a PI3K, with a reduced sensitivity to LY294002 and wortmannin, is involved in LPA-induced SC migration, in view of PI3K-C2α, a class II PI3K that was shown to be at least 10-times less sensitive to both PI3K inhibitors compared with class I PI3Ks (Domin et al., 1997). In addition, another class II PI3K, PI3K-C2β, has been reported to be crucial in LPA-dependent migration of human cell lines (Maffucci et al., 2005). These class II PI3Ks might also be involved in LPA-induced SC migration resulting in incomplete inhibition when LY294002 and wortmannin were used. Lack of inhibition of LPA-induced SC migration when SP600125, a specific JNK inhibitor, was used reveals a divergence in the signaling pathway downstream of Rac for LPA-induced SC migration as compared with NT-3- or NRG-induced migration (Yamauchi et al., 2008).

These results add to the previously reported functions for LPA signaling in SC survival, adhesion, and actin rearrangement (Weiner and Chun, 1999; Weiner et al., 2001) to include roles in embryonic SC migration, axonal segregation, and myelination in the PNS. These results also provide additional support for the phospholipid metabolism of LPA and biochemically related phosphatidic acid in the establishment, as well as the disruption, of peripheral myelination (Nadra et al., 2008). The prominent presence of LPA in hemorrhagic fluids may link prenatal bleeding events to disruption of normal peripheral nerve development, in view of LPA receptor-dependent CNS disruption associated with hypoxia (Herr et al., 2011) and fetal hydrocephalus (Yung et al., 2011), raising the possibility of similar mechanisms occurring in adult repair settings. In addition, the efficacy of fingolimod for the treatment of multiple sclerosis - fingolimod is metabolized into an analog of S1P - raises the prospect of potential therapeutics targeting peripheral nerves through lysophospholipid signaling (Choi et al., 2011; Cohen and Chun, 2011; Mutoh et al., 2012).

Acknowledgment

Grant sponsor: NIH; Grant numbers: NS048478 and MH051699 (to J.C.); Grant sponsor: Swiss National Science Foundation (to B.A.); Grant sponsor: National Research Foundation of Korea; Grant number: 20120123322 (to J.W.C.).

The authors thank G. Bokoch for providing plasmids encoding PAK1-PBD for pulldown experiments and honor of memory; B. Webb for assistance with HPLC/MS, M. Wood for assistance with electron microscopy; K. Spencer for assistance with MetaMorph image analysis, J. Birkenfeld for critical reading of the manuscript, and D. Letourneau Jones for editorial assistance.

References

Allard J, Barron S, Diaz J, Lubetzki C, Zalc B, Schwartz JC, Sokoloff P. 1998. A rat G protein-coupled receptor selectively expressed in myelin-forming cells. Eur J Neurosci 10:1045–1053.

Anliker B, Chun J. 2004. Lysophospholipid G protein-coupled receptors. J Biol Chem 279:20555–20558.

Anton ES, Weskamp G, Reichardt LF, Matthew WD. 1994. Nerve growth factor and its low-affinity receptor promote Schwann cell migration. Proc Natl Acad Sci USA 91:2795–2799.

Benard V, Bokoch GM. 2002. Assay of Cdc42, Rac, and Rho GTPase activation by affinity methods. Methods Enzymol 345:349–359.

Benninger Y, Thurnherr T, Pereira JA, Krause S, Wu X, Chrostek-Grashoff A, Herzog D, Nave KA, Franklin RJ, Meijer D, Brakebusch C, Suter U, Relvas JB. 2007. Essential and distinct roles for cdc42 and rac1 in the regulation of Schwann cell biology during peripheral nervous system development. J Cell Biol 177(6):1051–61.

Cervera P, Tirard M, Barron S, Allard J, Trottier S, Lacombe J, Daumas-Duport C, Sokoloff P. 2002. Immunohistological localization of the myelinating cell-specific receptor LP(A1). Glia 38:126–136.

Chan JR, Cosgaya JM, Wu YJ, Shooter EM. 2001. Neurotrophins are key mediators of the myelination program in the peripheral nervous system. Proc Natl Acad Sci USA 98:14661–14668.

Choi JW, Gardell SE, Herr DR, Rivera R, Lee CW, Noguchi K, Teo ST, Yung YC, Lu M, Kennedy G, Chun J. 2011. FTY720 (fingolimod) efficacy in an animal model of multiple sclerosis requires astrocyte sphingosine 1-phosphate receptor 1 (S1P1) modulation. Proc Natl Acad Sci USA 108:751–756.

Choi JW, Herr DR, Noguchi K, Yung YC, Lee CW, Mutoh T, Lin ME, Teo ST, Park KE, Mosley AN, Chun J. 2010. LPA receptors: subtypes and biological actions. Annu Rev Pharmacol Toxicol 50:157–186.

Cohen JA, Chun J. 2011. Mechanisms of fingolimod's efficacy and adverse effects in multiple sclerosis. Ann Neurol 69:759–777.

Contos JJ, Fukushima N, Weiner JA, Kaushal D, Chun J. 2000. Requirement for the lpA1 lysophosphatidic acid receptor gene in normal suckling behavior. Proc Natl Acad Sci USA 97:13384–13389.

Cosgaya JM, Chan JR, Shooter EM. 2002. The neurotrophin receptor p75NTR as a positive modulator of myelination. Science 298:1245–1248.

Domin J, Pages F, Volinia S, Rittenhouse SE, Zvelebil MJ, Stein RC, Waterfield MD. 1997. Cloning of a human phosphoinositide 3-kinase with a C2 domain that displays reduced sensitivity to the inhibitor wortmannin. Biochem J 326:139–147.

Fukushima N, Weiner JA, Chun J. 2000. Lysophosphatidic acid (LPA) is a novel extracellular regulator of cortical neuroblast morphology. Dev Biol 228: 6–18.

Garratt AN, Britsch S, Birchmeier C. 2000. Neuregulin, a factor with many functions in the life of a schwann cell. Bioessays 22:987–996.

Gomez-Sanchez JA, Lopez de Armentia M, Lujan R, Kessaris N, Richardson WD, Cabedo H. 2009. Sustained axon-glial signaling induces Schwann cell hyperproliferation, Remak bundle myelination, and tumorigenesis. J Neurosci 29:11304–11315.

Hecht JH, Weiner JA, Post SR, Chun J. 1996. Ventricular zone gene-1 (vzg-1) encodes a lysophosphatidic acid receptor expressed in neurogenic regions of the developing cerebral cortex. J Cell Biol 135:1071–1083.

Herr KJ, Herr DR, Lee CW, Noguchi K, Chun J. 2011. Stereotyped fetal brain disorganization is induced by hypoxia and requires lysophosphatidic acid receptor 1 (LPA1) signaling. Proc Natl Acad Sci USA 108:15444–15449.

Inoue M, Rashid MH, Fujita R, Contos JJ, Chun J, Ueda H. 2004. Initiation of neuropathic pain requires lysophosphatidic acid receptor signaling. Nat Med 10:712–718.

Ishii I, Ye X, Friedman B, Kawamura S, Contos JJ, Kingsbury MA, Yang AH, Zhang G, Brown JH, Chun J. 2002. Marked perinatal lethality and cellular signaling deficits in mice null for the two sphingosine 1-phosphate (S1P) receptors, S1P(2)/LP(B2)/EDG-5 and S1P(3)/LP(B3)/EDG-3. J Biol Chem 277:25152–25159.

Jessen KR, Mirsky R. 2005. The origin and development of glial cells in peripheral nerves. Nat Rev Neurosci 6:671–682.

Jessen KR, Mirsky R. 2008. Negative regulation of myelination: relevance for development, injury, and demyelinating disease. Glia 56:1552–1565.

Kim HAaR, N. 1997. A procedure for isolating Schwann cells developed for analysis of the mouse embryonic lethal mutation *NF1*. In: Juurlink BHEA, editor. Cell biology and pathology of myelin. New York: Plenum. pp 201–121.

Kupperman E, An S, Osborne N, Waldron S, Stainier DY. 2000. A sphingosine-1-phosphate receptor regulates cell migration during vertebrate heart development. Nature 406:192–195.

Lemke G. 2006. Neuregulin-1 and myelination. Sci STKE 2006:pe11.

Li Y, Gonzalez MI, Meinkoth JL, Field J, Kazanietz MG, Tennekoon GI. 2003. Lysophosphatidic acid promotes survival and differentiation of rat Schwann cells. J Biol Chem 278:9585–9591.

Li Y, Tennekoon GI, Birnbaum M, Marchionni MA, Rutkowski JL. 2001. Neuregulin signaling through a PI3K/Akt/Bad pathway in Schwann cell survival. Mol Cell Neurosci 17:761–767.

Li Z, Paik JH, Wang Z, Hla T, Wu D. 2005. Role of guanine nucleotide exchange factor P-Rex-2b in sphingosine 1-phosphate-induced Rac1 activation and cell migration in endothelial cells. Prostagland Other Lipid Mediat 76:95–104.

Lin ME, Rivera RR, Chun J. 2012. Targeted deletion of LPA5 identifies novel roles for lysophosphatidic acid signaling in development of neuropathic pain. J Biol Chem 287:17608–17617.

Little GJ, Heath JW. 1994. Morphometric analysis of axons myelinated during adult life in the mouse superior cervical ganglion. J Anat 184:387–398.

Lyons DA, Pogoda HM, Voas MG, Woods IG, Diamond B, Nix R, Arana N, Jacobs J, Talbot WS. 2005. erbb3 and erbb2 are essential for schwann cell migration and myelination in zebrafish. Curr Biol 15:513–524.

Maffucci T, Cooke FT, Foster FM, Traer CJ, Fry MJ, Falasca M. 2005. Class II phosphoinositide 3-kinase defines a novel signaling pathway in cell migration. J Cell Biol 169:789–799.

Mahanthappa NK, Anton ES, Matthew WD. 1996. Glial growth factor 2, a soluble neuregulin, directly increases Schwann cell motility and indirectly promotes neurite outgrowth. J Neurosci 16:4673–4683.

Malchinkhuu E, Sato K, Horiuchi Y, Mogi C, Ohwada S, Ishiuchi S, Saito N, Kurose H, Tomura H, Okajima F. 2005. Role of p38 mitogen-activated kinase and c-Jun terminal kinase in migration response to lysophosphatidic acid and sphingosine-1-phosphate in glioma cells. Oncogene 24:6676–6688.

Meintanis S, Thomaidou D, Jessen KR, Mirsky R, Matsas R. 2001. The neuron-glia signal beta-neuregulin promotes Schwann cell motility via the MAPK pathway. Glia 34:39–51.

Michailov GV, Sereda MW, Brinkmann BG, Fischer TM, Haug B, Birchmeier C, Role L, Lai C, Schwab MH, Nave KA. 2004. Axonal neuregulin-1 regulates myelin sheath thickness. Science 304:700–703.

Milner R, Wilby M, Nishimura S, Boylen K, Edwards G, Fawcett J, Streuli C, Pytela R, ffrench-Constant C. 1997. Division of labor of Schwann cell integrins during migration on peripheral nerve extracellular matrix ligands. Dev Biol 185:215–228.

Morris JK, Lin W, Hauser C, Marchuk Y, Getman D, Lee KF. 1999. Rescue of the cardiac defect in ErbB2 mutant mice reveals essential roles of ErbB2 in peripheral nervous system development. Neuron 23:273–283.

Mutoh T, Rivera R, Chun J. 2012. Insights into the pharmacological relevance of lysophospholipid receptors. Br J Pharmacol 165:829–844.

Nadra K, de Preux Charles AS, Medard JJ, Hendriks WT, Han GS, Gres S, Carman GM, Saulnier-Blache JS, Verheijen MH, Chrast R. 2008. Phosphatidic acid mediates demyelination in Lpin1 mutant mice. Genes Dev 22:1647–1661.

Nagai J, Uchida H, Matsushita Y, Yano R, Ueda M, Niwa M, Aoki J, Chun J, Ueda H. 2010. Autotaxin and lysophosphatidic acid1 receptor-mediated demyelination of dorsal root fibers by sciatic nerve injury and intrathecal lysophosphatidylcholine. Mol Pain 6:78.

Nave KA, Salzer JL. 2006. Axonal regulation of myelination by neuregulin 1. Curr Opin Neurobiol 16:492–500.

Nodari A, Zambroni D, Quattrini A, Court FA, D'Urso A, Recchia A, Tybulewicz VL, Wrabetz L, Feltri ML. 2007. Beta1 integrin activates Rac1 in Schwann cells to generate radial lamellae during axonal sorting and myelination. J Cell Biol 177:1063–1075.

Okabe M, Ikawa M, Kominami K, Nakanishi T, Nishimune Y. 1997. 'Green mice' as a source of ubiquitous green cells. FEBS Lett 407:313–319.

Rasi K, Hurskainen M, Kallio M, Staven S, Sormunen R, Heape AM, Avila RL, Kirschner D, Muona A, Tolonen U, Tanila H, Huhtala P, Soininen R, Pihlajaniemi T. 2010. Lack of collagen XV impairs peripheral nerve maturation and, when combined with laminin-411 deficiency, leads to basement membrane abnormalities and sensorimotor dysfunction. J Neurosci 30:14490–14501.

Taveggia C, Zanazzi G, Petrylak A, Yano H, Rosenbluth J, Einheber S, Xu X, Esper RM, Loeb JA, Shrager P, Chao MV, Falls DL, Role L, Salzer JL. 2005. Neuregulin-1 type III determines the ensheathment fate of axons. Neuron 47: 681–694.

Van Leeuwen FN, Olivo C, Grivell S, Giepmans BN, Collard JG, Moolenaar WH. 2003. Rac activation by lysophosphatidic acid LPA1 receptors through the guanine nucleotide exchange factor Tiam1. J Biol Chem 278:400–406.

Voyvodic JT. 1989. Target size regulates calibre and myelination of sympathetic axons. Nature 342:430–433.

Weiner JA, Chun J. 1999. Schwann cell survival mediated by the signaling phospholipid lysophosphatidic acid. Proc Natl Acad Sci USA 96:5233–5238.

Weiner JA, Fukushima N, Contos JJ, Scherer SS, Chun J. 2001. Regulation of Schwann cell morphology and adhesion by receptor-mediated lysophosphatidic acid signaling. J Neurosci 21:7069–7078.

Weiner JA, Hecht JH, Chun J. 1998. Lysophosphatidic acid receptor gene vzg-1/lpA1/edg-2 is expressed by mature oligodendrocytes during myelination in the postnatal murine brain. J Comp Neurol 398:587–598.

Woldeyesus MT, Britsch S, Riethmacher D, Xu L, Sonnenberg-Riethmacher E, Abou-Rebyeh F, Harvey R, Caroni P, Birchmeier C. 1999. Peripheral nervous system defects in erbB2 mutants following genetic rescue of heart development. Genes Dev 13:2538–2548.

Yamauchi J, Chan JR, Shooter EM. 2003. Neurotrophin 3 activation of TrkC induces Schwann cell migration through the c-Jun N-terminal kinase pathway. Proc Natl Acad Sci USA 100:14421–14426.

Yamauchi J, Chan JR, Shooter EM. 2004. Neurotrophins regulate Schwann cell migration by activating divergent signaling pathways dependent on Rho GTPases. Proc Natl Acad Sci USA 101:8774–8779.

Yamauchi J, Miyamoto Y, Chan JR, Tanoue A. 2008. ErbB2 directly activates the exchange factor Dock7 to promote Schwann cell migration. J Cell Biol 181:351–365.

Yamauchi J, Miyamoto Y, Tanoue A, Shooter EM, Chan JR. 2005. Ras activation of a Rac1 exchange factor, Tiam1, mediates neurotrophin-3-induced Schwann cell migration. Proc Natl Acad Sci USA 102:14889–14894.

Yung YC, Mutoh T, Lin ME, Noguchi K, Rivera RR, Choi JW, Kingsbury MA, Chun J. 2011. Lysophosphatidic acid signaling may initiate fetal hydrocephalus. Sci Transl Med 3:99ra87.